The 1983 Institute of Metals Lecture
The Metallurgical Society of AIME

The Mechanical Properties of Cellular Solids

M. F. ASHBY
R. F. Mehl Medalist

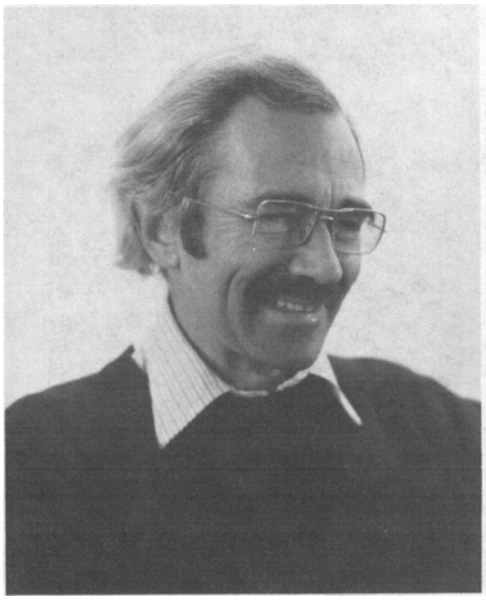

The mechanical properties (elastic, plastic, creep, and fracture) of cellular solids or foams are related to the properties of the cell wall material and to the cell geometry. The properties are well described by simple formulae. Such materials occur widely in nature and have many potential engineering applications.

FOREWORD

THIS paper was presented at a meeting convened to renew the memory of Professor Robert Franklin Mehl. It is easy to forget that the field in which we, most of us, work — the broad field of Materials Science — is not very old. He was one of the great pioneers, one of the first to explore and map out the origins of structure in materials and the way it controls properties. The work described below, and, above all, the approach to it, is in the tradition of which he was one of the founders.

The Institute of Metals Lecture was established in 1921, at which time the Institute of Metals Division was the only professional Division within the American Institute of Mining and Metallurgical Engineers. It has been given annually since 1922 by distinguished men from this country and abroad. Beginning in 1973 and thereafter, the person selected to deliver the lecture will be known as the "Institute of Metals Division Lecturer and R. F. Mehl Medalist" for that year.

Dr. ASHBY received his B. A., M. A., and Ph. D. degrees at the University of Cambridge, England. He has been the Editor of *Acta Metallurgica* since 1974 and is an Honorary Research Fellow at Harvard University. Dr. Ashby has served as Chairman of the NATO Study Group on Materials Resources and was a member of the National Economic Development Council Study Group on Materials in the British Economy. He was elected a Fellow of the Royal Society in 1979 and is the recipient of the L. B. Pfeil Medal and the Rosenhain Medal of the Metals Society.

A large portion of this work was done in collaboration with Dr. L. J. Gibson. Dr. Gibson is now Assistant Professor of Structural Engineering, University of British Columbia.

I. INTRODUCTION

When modern man builds large load-bearing structures, he uses dense solids: steel, concrete, glass. When nature does the same,* she generally uses cellular materials: wood, bone, coral. There must be good reasons for this. It is, almost certainly, that cellular materials permit the simultaneous optimization of stiffness, strength, and overall weight in a given application. Cellular solids are nature's equivalent of the I-beam.

*To give an idea of the scale of some natural "structures", a large dinosaur was about the length and weight of a 25-seater aircraft; a large redwood tree is about the height of a 30-floor building (100 m) and weighs around 2500 tonnes.

Man-made foams are common enough, of course: cushioning, insulation, padding, packaging are all functions filled by cellular solids. Nature uses them in these ways, too: orange peel to protect the orange, cork bark to insulate the tree. But while nature has, for aeons, used cellular materials to support large loads, man, until recently, has used only wood — a natural cellular solid — in this role. His ability to design and optimize his own cellular structures is still limited.

In this article, I would like to summarize the understanding — some of it old, some more recent — of the mechanical behavior of cellular solids. The engineering potential of cellular materials is considerable, but its realization requires new and innovative methods of design, unfamiliar to traditional engineers.

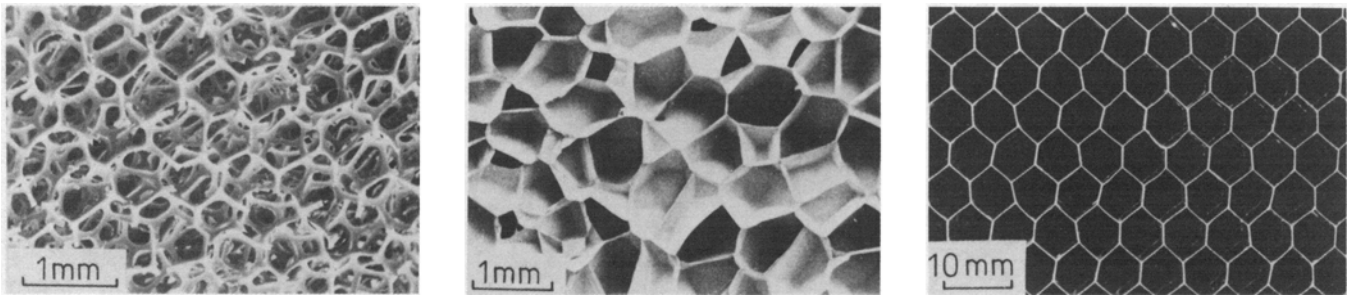

(a) (b) (c)

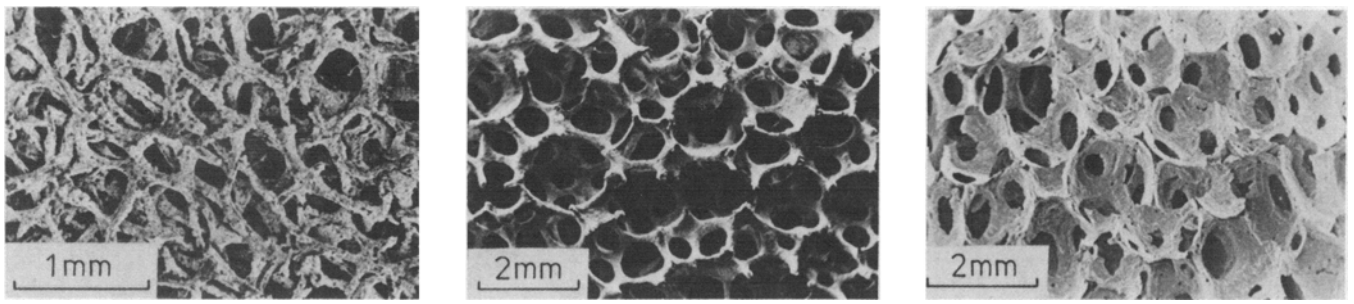

(d) (e) (f)

Fig. 1 — Man-made foams: (*a*) an open-cell polyurethane; (*b*) a closed-cell polyurethane; (*c*) aluminum honeycomb; (*d*) copper; (*e*) mullite; (*f*) zirconia.

II. THE STRUCTURE OF CELLULAR SOLIDS

Making foams is not difficult. Most polymers can be foamed easily, and techniques exist for doing the same thing with ceramics and glasses. Even metals can be formed into foams.

A. *Isotropic and Anisotropic, Open, and Closed-Cell Foams*

What do they look like? Figure 1 shows man-made cellular solids: polymers, ceramics, and metals; Figure 2 shows natural cellular materials: cork, wood, sponge, coral, bone, and cuttle bone. They show that some foams are almost *isotropic*, meaning that their structure and their properties have no directionality. Others are *anisotropic*: their structure is axisymmetric (like cork) or orthotropic (like wood); and their properties reflect this. Man-made foams tend to be almost isotropic. Natural cellular solids are rarely so; a single piece of cork or bone differs in strength and stiffness by a factor of 2 or more along two directions at right angles. Wood is more anisotropic still: many woods are 10 times stiffer and stronger when loaded along the grain than across it. So we cannot ignore the directionality of cell structures;

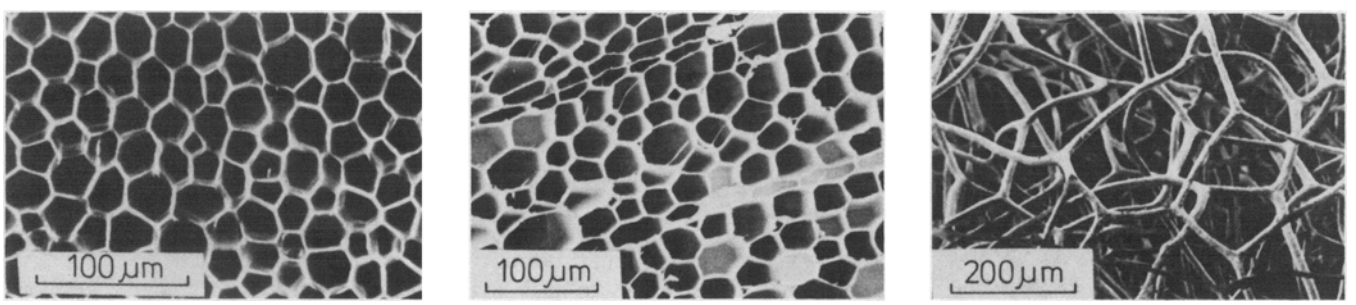

(a) (b) (c)

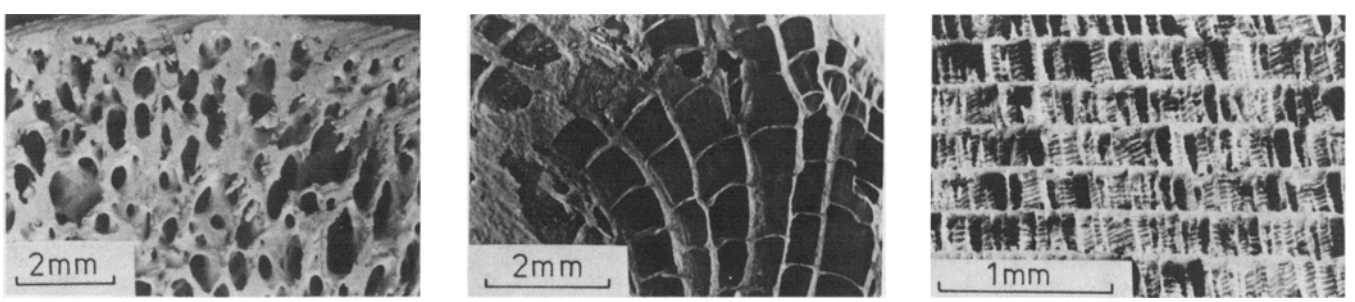

(d) (e) (f)

Fig. 2 — Natural foams: (*a*) cork; (*b*) balsa wood; (*c*) sponge; (*d*) bone; (*e*) coral; (*f*) cuttle bone.

and it is a feature which can be built into man-made foams and exploited in engineering design (as it now is in design with wood).

The pictures illustrate a second distinction. Some foams have *closed cells* (like a soap foam): the solid material is distributed in little plates which form the faces of the cells. Others have *open cells* (like a sponge): the solid material is distributed in little columns or beams which form the cell edges. The mechanical properties reflect, to some extent, this distribution. In reality, most man-made foams, even those with closed cell faces, behave like open-celled foams because surface tension draws much of the solid material into the cell edges during manufacture.

These are the finer distinctions of structure. We have overlooked the most important aspect of the structure: the *relative density*, ρ/ρ_s, where ρ is the density of the foam and ρ_s that of the solid of which the foam is made. The mechanical properties of foams depend, above all else, on the relative density. It can vary from 1 to as little as 0.01. The familiar foamed plastics used for packaging have a relative density of around 0.05.

B. *Deformation Mechanisms and Idealized Foam Structures*

Detailed studies[1-4] of model foams have identified four *deformation modes*: linear elasticity, nonlinear elasticity, plastic collapse, and various sorts of fracture. The studies used two-dimensional hexagonal cells, like those in the diagrams shown later in this paper. A hexagonal network is a good starting point because the modes of deformation correspond to those of three-dimensional foams, yet the geometry is simple enough that a complete analysis is practical. The understanding derived from the two-dimensional models has provided the foundation for the analysis of the more complicated problem presented by real, three-dimensional foams[4-10] given below.

In the analysis, the three-dimensional structure of the foam must be included. It is idealized, without loss of physically important features, in the models shown in Figure 3. The open-cell foam is modeled as a cubic array of members of length l and square section of side t. Adjoining cells are staggered so that members meet at mid-points. The relative density of the cell, ρ/ρ_s, (where ρ_s is the density of the cell wall material) is then given by:

$$\frac{\rho}{\rho_s} \propto \left(\frac{t}{l}\right)^2 \qquad [1]$$

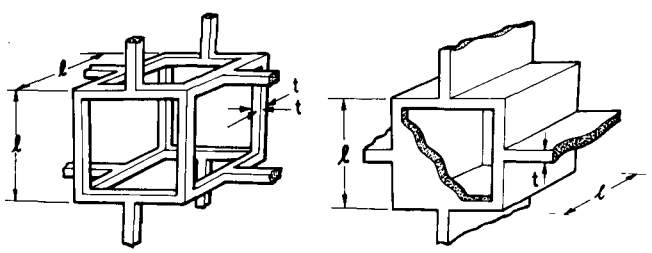

Fig. 3 — The 3-dimensional structure of open- and closed-cell foams, idealized. The cell walls meet so that loads cause bending moments to be applied to the cell walls. Most foams behave like the open-cell foam.

and the second moment of the section of a member (which we need later) is given by:

$$I = \frac{t^4}{12} \qquad [2]$$

A closed-cell foam is modeled similarly. The square struts are replaced by square plates of side l and thickness t. Adjoining cells are again staggered. Then:

$$\frac{\rho}{\rho_s} \propto \frac{t}{l}$$
$$I = \frac{lt^3}{12} \qquad [3]$$

As pointed out earlier, most foams behave more like the first model, because surface tension concentrates material into the cell edges during their manufacture. We will use it as the basis of the calculations given below, which treat isotropic foams. Refinements, results for the second model, and the generalizations to nonisotropic foams are given elsewhere.[1,2,10] Symbols are defined in Table I.

III. MECHANICAL PROPERTIES

When a foam is compressed, the stress-strain curve shows three regions (Figure 4). At low strains, the foam deforms in a *linear-elastic* way; there is then a plateau of *deformation at almost constant stress*; and finally there is a region of *densification* as the cell walls crush together. The extent of each region depends on relative density ρ/ρ_s. Elastic foams, plastic foams, and even brittle foams all have three-part stress-strain curves like this, though the mechanism causing the plateau is different in each case.

The deformation of a regular, two-dimensional foam like that sketched in Figure 5 can be analyzed with precision. It is far more difficult to do the same analysis for a three-dimensional foam, because the response is an average of

Table I. Symbols and Units

ρ	Density of foam (kg/m^3)
ρ_s	Density of cell-wall material (kg/m^3)
E	Young's Modulus of foam (MPa)
E_s	Young's Modulus of cell-wall material (MPa)
σ^*_{el}	Elastic collapse stress of elastomeric foam (MPa)
σ^*_{pl}	Plastic collapse stress of plastic foam (MPa)
σ_y	Yield strength of cell-wall material (MPa)
$\dot{\varepsilon}$	Strain rate (s^{-1})
$\dot{\varepsilon}_0, \sigma_0, n$	Creep constants (s^{-1}, MPa, –)
σ^*_f	Crushing strength of brittle foam (MPa)
σ_f	Modulus of rupture of cell-wall material (MPa)
K_{IC}	Fracture toughness of foam (MPa m$^{1/2}$)
t	Cell wall thickness (m)
l	Cell size or cell wall length (m)
a	Half-length of crack (m)
I	Second moment of area of cell wall (m^4)
F	Force acting on a cell wall (N)
F_{cr}	Euler buckling load for cell wall (N)
M_p	Fully plastic moment of cell wall (Nm)
M_f	Moment which will just fracture cell wall (Nm)
C_1 to C_8	Dimensionless constants
B_1 to B_8	Dimensionless constants

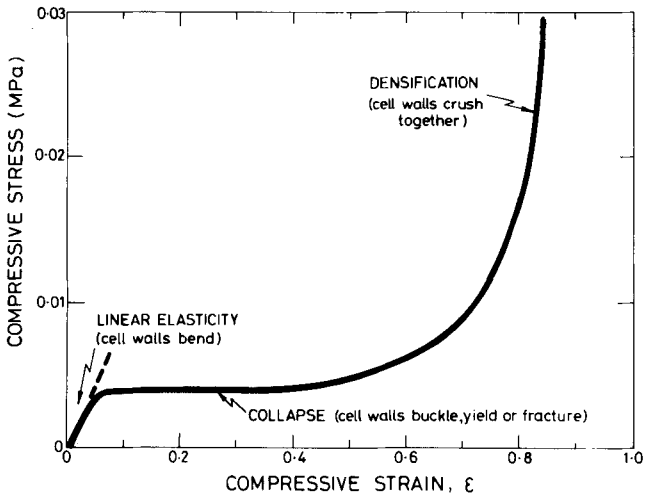

Fig. 4—The typical shape of the stress-strain curve for a foam.

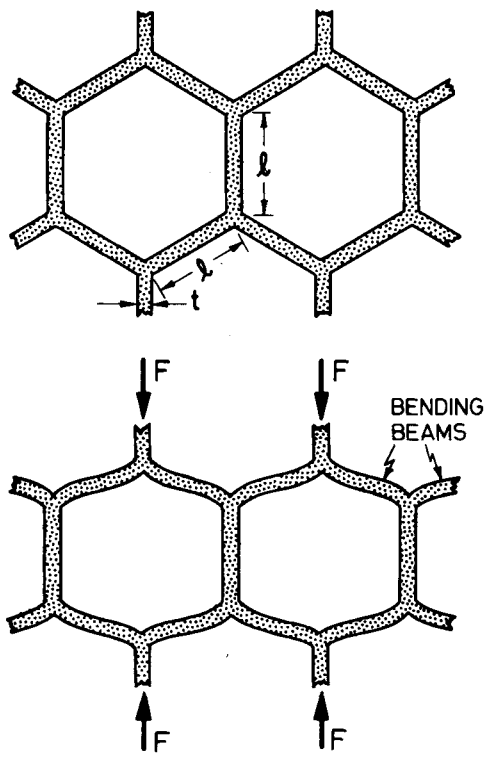

Fig. 5—The linear-elastic deformation of a foam: the cell walls bend so that the bending deflection δ is proportional to the force F.

that of cell walls of random orientation in space, and with a distribution of length l and section t^2. It is better to use the dimensional argument given below, and then rely on experiment to determine a single, unknown constant of proportionality. This method, which we have used to analyze many properties of foams, will become clearer as it is applied in the following sections.

A. *Linear Elastic Properties*

When a foam is loaded, the cell walls at first *bend*.[2,3,7,9,10] Figure 5 shows this bending for the two-dimensional model; the same bending deformation occurs in three-dimensional foams. A force F, applied as shown, causes the nonvertical beams to deflect by δ, which is calculated from single beam theory as:

$$\delta = \frac{C_1 F l^3}{12 E_s I} \qquad [4]$$

Here C_1 is a resolution factor which depends only on the cell geometry, and E_s is the Young's modulus of the solid cell wall material. For the open-cell foam of Figure 3(a) the stress is proportional to F/l^2, the strain to δ/l. The second moment of area, I, is proportional to t^4 (Eq. [2]) giving:

$$E \propto E_s \frac{t^4}{l^4}$$

Using Eq. [1] for the density, we find:

$$\frac{E}{E_s} = C_2 \left(\frac{\rho}{\rho_s}\right)^2 \qquad [5]$$

where C_2 is a constant. The shear modulus scales in a similar way, because shear deformation in a foam also causes simple bending of the cell walls.[2]

Data are compared with Eq. [5] in Figure 6. It shows Young's moduli for polymeric and ceramic foams plotted against ρ/ρ_s on logarithmic scales. The full line is a plot of Eq. [5] with $C_2 = 1$; it gives a good description of a wide

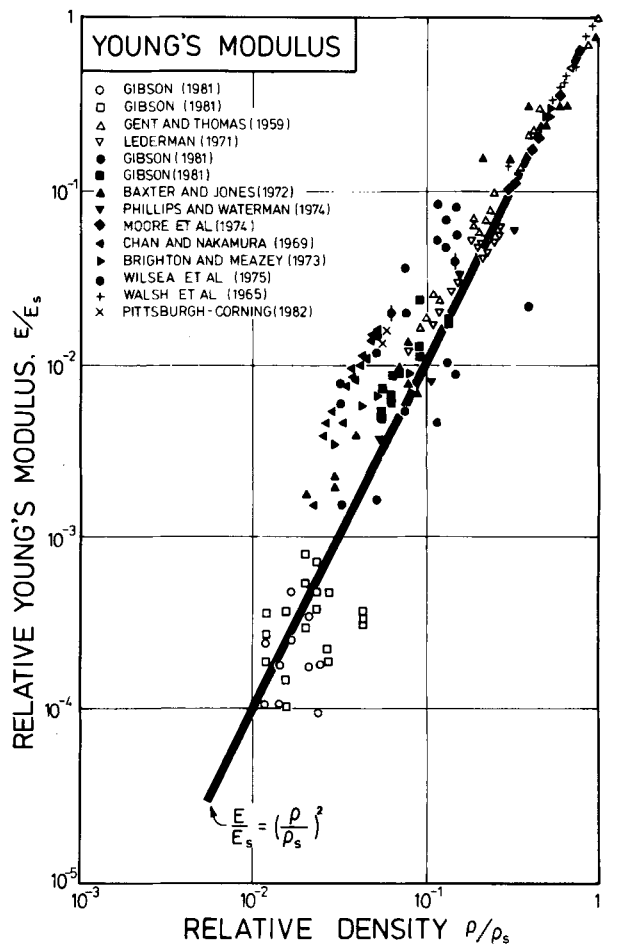

Fig. 6—The relative Young's E/E_s, plotted against relative density, ρ/ρ_s. Open symbols represent open-cell polymer foams; shaded symbols represent closed-cell polymer foams; crosses are ceramic and glass foams. (The references, in order, are: 1, 5, 8, 11–17; normalizing constants in Table II.)

range of materials and densities. Note that the modulus falls rapidly as the volume of void space in the foam increases. The *range* of moduli practically available by foaming is large: it spans a factor of 10^4. The modulus is important in the design of load-bearing structures which incorporate foams (sandwich panels, for example).

B. *Nonlinear Elastic Behavior*

Linear elasticity, of course, is limited to small strains, typically 5 pct in compression, rather more in tension. Elastomeric foams can be compressed far beyond this point. The deformation is still recoverable (and thus elastic), but is nonlinear; it is caused by the *elastic buckling* of the columns or plates which make up the cell edges or walls[2,5,6,10] as shown in Figure 7, giving the plateau of the stress-strain curve* (Figure 4). It is exploited in cushions and packaging to give a restoring force (which we now calculate) which is independent of displacement.

*Several authors[3,9,14,19,20] studying the collapse of rigid foams sought to interpret their results as elastic buckling. Their calculations are in the spirit of that given here, but are inappropriate to the materials they studied.

The critical load at which a column of length l, Young's modulus E_s, and second moment of area I buckles is given by Euler's formula:

$$F_{cr} = \frac{n^2\pi^2 E_s I}{l^2} \qquad [6]$$

The constant n^2 describes the degree of constraint at the ends of the column. If this load is reached for a layer of cells spanning the section, they will buckle, initiating the *elastic collapse* of the foam. For the three-dimensional open-cell foam of Figure 3, the stress σ_{el}^* at which this occurs is proportional to F_{cr}/l^2, so that:

$$\sigma_{el}^* = n^2\pi^2 \frac{E_s I}{l^4}$$

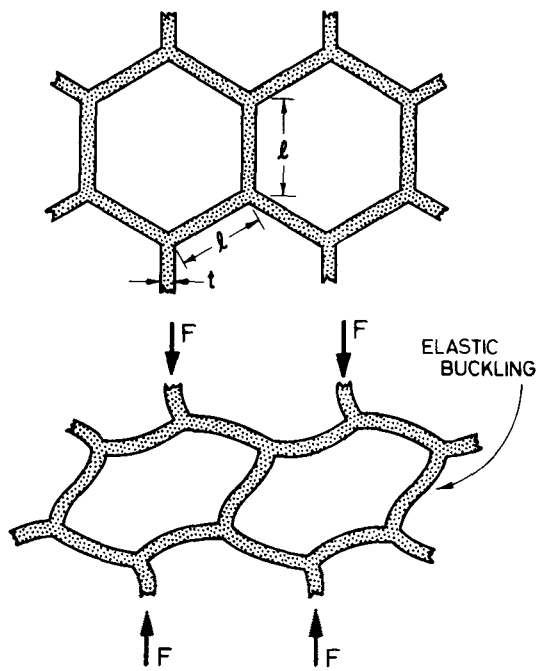

Fig. 7—The nonlinear deformation of a foam: the cell walls buckle, giving large deformation at an almost constant stress.

Using Eqs. [1] and [2] we obtain:

$$\frac{\sigma_{el}^*}{E_s} = C_3\left(\frac{\rho}{\rho_s}\right)^2 \qquad [7]$$

valid for relative densities below 0.3 because, at higher densities, the cell walls are too short and stocky to buckle.

Data for σ_{el}^* for elastomeric foams are compared with Eq. [7] in Figure 8. They are well fitted by the equation with $C_3 = 0.05$. Like the modulus, the elastic collapse stress spans a wide range: for a given material, a range of 10^4 is accessible. This is important for the design of cushions, padding, and packaging.

C. *Plastic Yielding*

Cellular materials can collapse by other mechanisms. If the cell-wall material is *plastic* (as are metals and many polymers), then the foam as a whole shows plastic behavior. It is exploited in crash barriers and energy absorbing systems.

Plastic collapse occurs when the moment exerted on the cell walls by the force F exceeds the fully plastic moment, creating plastic hinges[2,10,21,22] as shown in Figure 9. For a beam of square section of side t, the fully plastic moment is:

$$M_p = \frac{1}{4}\sigma_y t^3 \qquad [8]$$

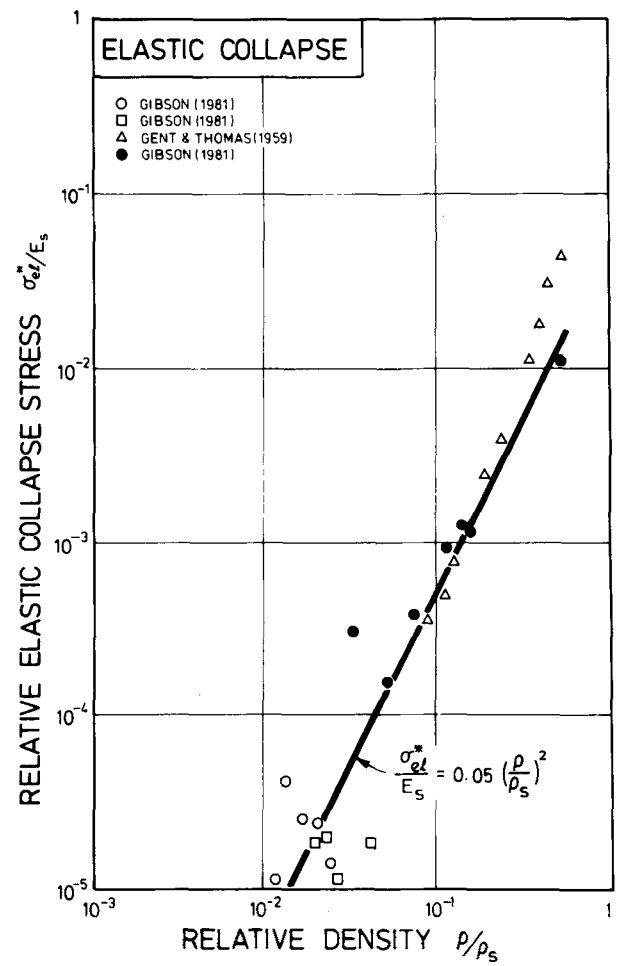

Fig. 8—The relative elastic collapse stress, σ_{el}^*/E_s, plotted against relative density, ρ/ρ_s. Open symbols represent open-cell polymer foams; shaded symbols represent closed-cell polymer foams. (The references, in order, are: 1, 5; normalizing constants in Table II.)

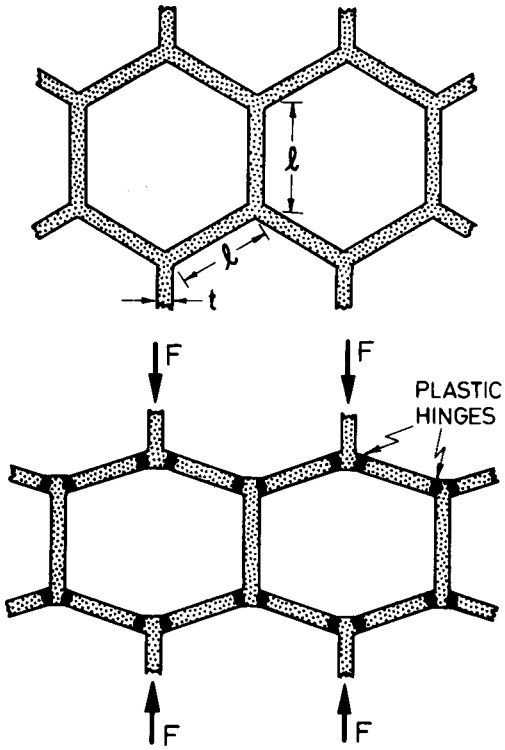

Fig. 9—The yielding of a plastic foam: the fully plastic moment of the cell wall is exceeded, giving large deformation at an almost constant stress σ_{pl}^*.

If a force F acts with a component normal to a beam of length l, the maximum bending moment is proportional to Fl. The stress on the foam, as before, is proportional to F/l^2. Combining these results we find the plastic collapse stress of the foam to be:

$$\sigma_{pl}^* \propto \frac{M_p}{l^3}$$

Using Eq. [1] we obtain:

$$\frac{\sigma_{pl}^*}{\sigma_y} = C_4\left(\frac{\rho}{\rho_s}\right)^{3/2} \qquad [9]$$

Data for the plastic deformation and for the plastic indentation of foams (discussed next) are plotted in Figure 10. They are well fitted by Eq. [9] with $C_4 = 0.3$ for relative densities of less than one-third (at higher densities the cell edges are too short and stocky to bend plastically). The plastic collapse stress can be "tailored", by choosing a foam of the right density, over a range of 10^3. It is of primary importance in the design of crash padding and energy-absorbing foams.

D. *Plastic Indentation*

Unlike dense solids, which are incompressible when deformed plastically to large strains, foams change their volume when compressed. The cells of the foam collapse as the foam is squeezed, so that axial compression produces almost no lateral spreading. (Poisson's ratio for the plastic compression of low density foam is, typically, 0.04.[1,10,24,25]) Such foams yield plastically under a multiaxial state of stress when the maximum principal stress, not the octahedral shear stress, reaches the critical value σ_{pl}^* calculated in the last section.

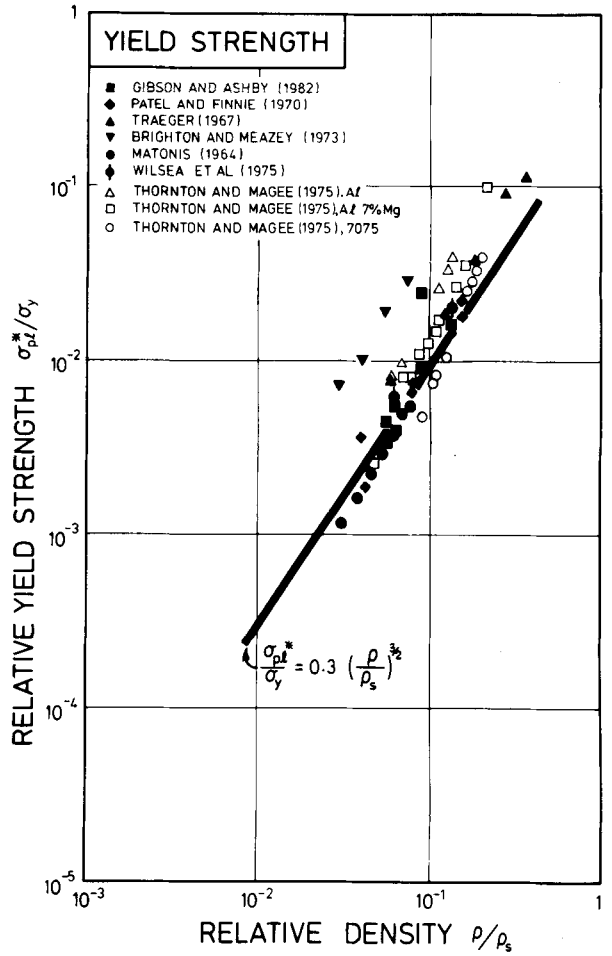

Fig. 10—The relative plastic collapse stress, σ_{pl}^*/σ_y, plotted against relative density, ρ/ρ_s. Open symbols are for metal foams; shaded symbols are for closed-cell polymer foams. (The references, in order, are 10, 3, 23, 15, 19, 16, 21; normalizing constants in Table II.)

Because of this, the indentation hardness of a foam is lower than that of a dense solid of the same yield stress: elements of the foam, compressed beneath the indenter, do not expand, and so are not constrained by the surrounding material in the same way that elements in a dense solid are. An analysis of the problem[16] shows that, for relative densities less than about 0.3, the indentation pressure, or "hardness" H of the foam is simply:

$$H = \sigma_{pl}^* \qquad [10]$$

(instead of the result $H = 3\sigma_y$ for a dense solid). Two experimental studies[16,24] confirm this result. The data from the second study are included in Figure 10.

E. *Creep*

At temperatures above about $0.3\,T_M$ (where T_M is the melting point), metals and ceramics deform by *creep*: slow extension or compression under constant load. Polymers creep, too, particularly once the temperature exceeds the glass temperature T_g. Foams made of these materials, too, will creep. Let the creep rate $\dot{\varepsilon}$ of the cell wall material be described by:

$$\dot{\varepsilon} = \dot{\varepsilon}_0\left(\frac{\sigma}{\sigma_0}\right)^n \qquad [11]$$

where $\dot{\varepsilon}_0$, σ_0, and n are creep constants. A beam of length l, thickness t, and width b, made of such a material, deflects at the rate:

$$\dot{\delta} \propto \frac{\dot{\varepsilon}_0 l}{(n+2)}\left(\frac{2l}{t}\right)^{n+1}\left\{\frac{2n+1}{2n}\frac{F}{bt\sigma_0}\right\}^n \qquad [12]$$

As before, for an open cell foam (Figure 3(a)), the load F is proportional to σl^2, and the strain-rate of the foam, $\dot{\varepsilon}$, is proportional to $\dot{\delta}/l$. Expressing t/l in terms of the relative density ρ/ρ_s (Eq. [1]) for $b = t$, we obtain:

$$\frac{\dot{\varepsilon}}{\dot{\varepsilon}_0} = C_5\frac{(2n+1)^n}{(n+2)n^n}\left(\frac{C_6\sigma}{\sigma_0}\right)^n\left(\frac{\rho_s}{\rho}\right)^{(3n+1)/2} \qquad [13]$$

where C_5 and C_6 are constants. This result correctly reduces to the linear elastic relation (Eq. [5]) when $n = 1$ (set $\sigma/\dot{\varepsilon} = E$ and $\sigma_0/\dot{\varepsilon}_0 = E_s$), from which we find that $C_5 = 1$. It also reduces to the solution for plastic collapse of the foam (Eq. [9]) when $n = \infty$ and $\sigma_0 = \sigma_y$, from which we find that $C_6 = 1.25$.

Although metal foams have been tested in the creep range,[22] the data are not complete enough to allow a test of Eq. [13]. It is valid for relative densities of less than 0.3, and has application whenever such foams carry steady loads at temperatures at which creep is possible.

F. *The Crushing Strength*

Brittle foams (ceramics and certain rigid polymers) collapse by yet other mechanisms: brittle crushing in compression[26] and brittle fracture in tension.[27,28] The low crushing strength of refractory brick (a cellular solid) limits the loads that can be applied to it; and the low fracture toughness of foams can cause problems when they carry tensile loads, as they do in sandwich panels.

Let the modulus of rupture* of the cell-wall material be σ_f. A cell wall will then fail (Figure 11) when the moment acting on it exceeds:

$$M_f = \frac{1}{6}\sigma_f t^3 \qquad [14]$$

As before, a force F, acting with a component normal to the wall of length l, exerts a moment which is proportional to Fl. The stress on the foam, as before, is proportional to F/l^2. Combining these results we find that collapse by crushing will occur at the stress:

$$\sigma_f^* \propto \frac{M}{l^3} \propto \sigma_f\left(\frac{t}{l}\right)^3$$

Using Eq. [1], we obtain:

$$\frac{\sigma_f^*}{\sigma_f} = C_7\left(\frac{\rho}{\rho_s}\right)^{3/2} \qquad [15]$$

There are few experimental measurements of the crushing of brittle foams. The limited data,[18,22] shown in Figure 12, are insufficient to give confidence that Eq. [15] is a good description. But certain other observations do suggest that

*The modulus of rupture of an elastic beam, loaded in bending, is the maximum surface stress in the beam at the instant of failure. The maximum stress is related to the moment by Eq. [14]. The modulus of rupture for a brittle solid is often close to the tensile fracture strength.

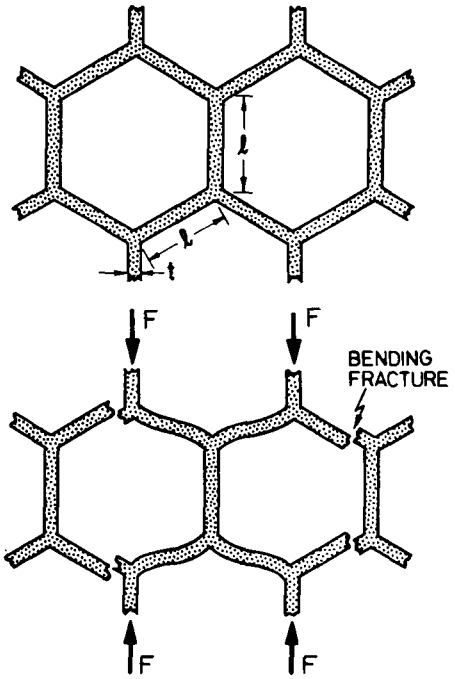

Fig. 11—The crushing of a brittle foam: the modulus of rupture of the cell walls is exceeded, causing them to fracture.

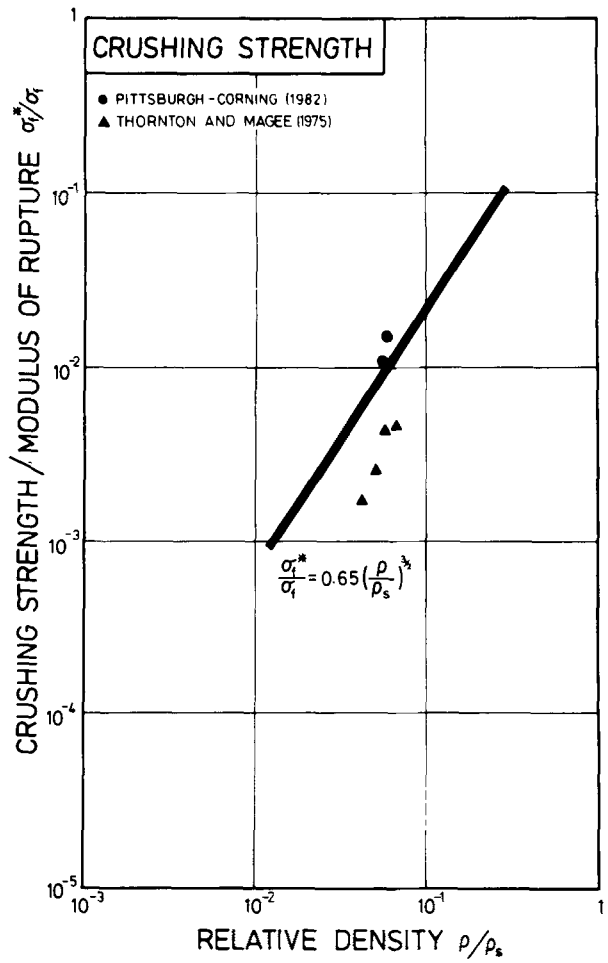

Fig. 12—The relative crushing strength, σ_f^*/σ_f, plotted against relative density ρ/ρ_s, for brittle foams. (The references, in order, are: 18, 22; normalizing constants in Table I.)

the model has the correct physical ingredients. First (and remarkably) the tensile and compressive fracture stress of unnotched foams should, according to the model, be equal (for brittle *solids*, the crushing strength is roughly 10 times the tensile strength). Measurements on foamed[18] glasses show that this is so. And, second, an extension of the model to describe crack propagation, and to predict the fracture toughness of foams, describes data well. This extension is described next.

G. *The Tensile Fracture Strength*

Compressive fracture is insensitive to defects—such things as flaws, cracks, or a few exceptionally large cells. But this is not so for tensile fracture. A completely unflawed sample, it is true, should sustain a tensile stress as high as that given by Eq. [15] before failing. But if it contained a crack or flaw, then the stress concentration it induces will fracture cell walls locally, extending the flaw and leading to sudden fracture (Figure 13).

When a brittle foam is loaded, the cell walls at first deform elastically. The load is transmitted through the foam as a set of discrete forces and moments acting on cell walls. But since the foam is *linear* elastic until the cell walls buckle, the average force and moment on a given cell wall can be calculated from the stress field in the equivalent linear-elastic continuum. We solve the discrete problem by taking the solution of the equivalent continuum problem (just as we do on a smaller scale in replacing the discrete bonds between atoms by a continuum) and using it to calculate the forces and moments on the discrete cell walls.

A crack of length a in an elastic solid, lying normal to a remote tensile stress σ^∞, creates a singular stress field:

$$\sigma = \frac{\sigma^\infty \sqrt{\pi a}}{\sqrt{2\pi r}} \qquad [16]$$

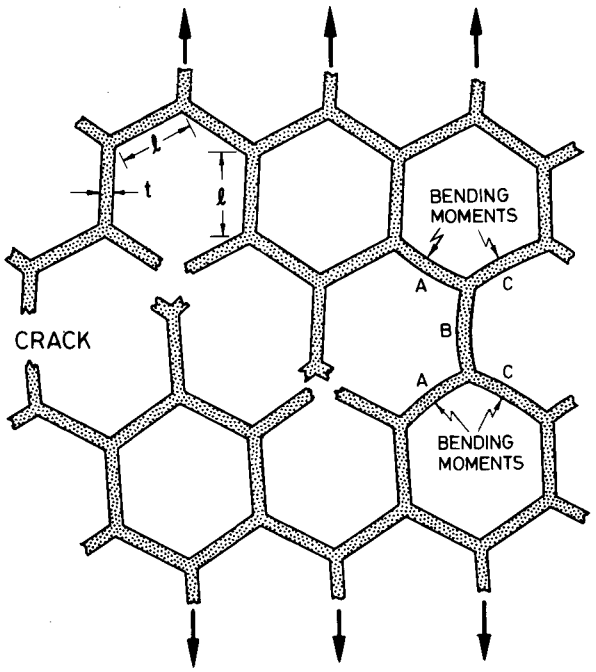

Fig. 13—Mode 1 crack propagation in a brittle foam: the field of the crack subjects cell walls to a bending moment and to tension. When the breaking strength of the cell wall is exceeded, the crack propagates.

at a distance r from its tip. Consider the first unbroken cell wall, which we take to be $l/2$ beyond the tip; it is subjected to a force:

$$F \propto \sigma l^2$$

where

$$\sigma = \sigma^\infty \sqrt{a/l}$$

This exerts a bending moment on the walls marked A and C, and bending moment plus a tensile stress on the wall

Table II. Properties of Cell-Wall Materials

Reference	Material	ρ_s (Kg m^{-2})	E_s (MPa)	σ_y (MPa)	σ_f (MPa)
Baxter and Jones[11]	expanded polystyrene	1020[11]	2650[11]	—	
Brighton and Meazey[15]	expanded polyvinyl chloride	1400[29,30]	3000[29,30]	49[29,30]	
Chan and Nakamura[14]	extruded polystyrene	1050[14]	1400[14]	—	
Gent and Thomas[5]	rubber latex foam	—	2.64[5]	—	
Gibson and Ashby[10]	open-cell flexible polyurethane	1200[29]	45[31]	—	
Gibson and Ashby[10]	closed-cell flexible cross-linked polyethylene	910[32]	200[32]	—	
Gibson and Ashby[10]	closed-cell rigid polyurethane	1200[29]	1600[3]	127[31]	
Lederman[8]	rubber latex foam	—	—	—	
Matonis[19]	rigid polystyrene	1050[29]	1380[19]	79[19]	
Moore *et al.*[13]	polypropylene copolymer	902[33]	1130[33]	—	
	polystyrene acrylonitrile	1065[13]	3670[13]	—	
Patel and Finnie[3]	rigid polyester-based polyurethane	1230[3]	1600[3]	127[3]	
Phillips and Waterman[12]	rigid polyurethane	1200[29]	1600[3]	—	
Traeger[23]	rigid polyurethane foam	1200[29]	1600[3]	127[3]	
Wilsea *et al.*[16]	rigid polyurethane	1200[29]	1600[3]	127[3]	127[3]
McIntyre and Anderton[27]	rigid polyurethane	1200[29]	1600[3]	127[3]	127
Fowlkes (1974)[28]	rigid polyurethane	1200[29]	1600[3]	127[3]	127
Thornton and Magee[21]	aluminum			52.2	—
	Al 7 pct Mg	2700[17]	69000	229	—
	Al 7075			342	
Thornton and Magee[22]	Zn at −196 °C	5200	43000	—	207[22]
Walsh *et al.*[17]	glass	2511[17]	75000[17]	—	
Pittsburgh-Corning[18]	glass	2500[34]	7000[34]	—	

marked B (Figure 13). If, as before, the walls fail when the moment, proportional to F, exceeds the fracture moment given by Eq. [14], then the crack advances. Assembling these results gives:

$$\sigma^{\infty} \propto \frac{t^3}{l^3} \frac{\sigma_f}{\sqrt{a/l}}$$

where σ_f, as before, is the modulus of rupture of the cell wall. Using Eq. [1] we obtain:

$$\sigma^{\infty} = C_8 \left(\frac{\rho}{\rho_s}\right)^{3/2} \frac{\sigma_f}{\sqrt{a/l}} \qquad [17]$$

where σ^{∞} is the remote stress which will cause the crack to propagate. The equation is valid only when $a > l$ (otherwise there is no crack).

The result is just what would be expected. The fracture strength equals that for the unnotched material (Eq. [15]) if the crack size is equal to the cell size. In an open-cell foam, a wall is either broken or it is not. If the crack size is less than the cell size, no cell walls are broken and the foam is undamaged. Comparing Eq. [17] with the definition of K_{IC} (the plane-strain toughness) for a through-crack in an infinite sheet:

$$K_{IC} = \sigma^{\infty} \sqrt{\pi a}$$

we find:

$$\frac{K_{IC}}{\sigma_f \sqrt{\pi l}} = C_8 \left(\frac{\rho}{\rho_s}\right)^{3/2} \qquad [18]$$

Data for crack propagation in a brittle polymeric foam are plotted in Figure 14. Eq. [18], with $C_8 = 0.65$, gives a good description of the data. Unlike all the other properties, K_{IC} depends on cell size. This, too, is expected: K_{IC} contains a dimension of length; the only lengths which enter the problem are the cell size l and the wall thickness t, but that is related to l through the relative density ρ/ρ_s (Eq. [1]). The result is important whatever forms are used in load-bearing applications in which tensile forces appear — as they do in sandwich panels.

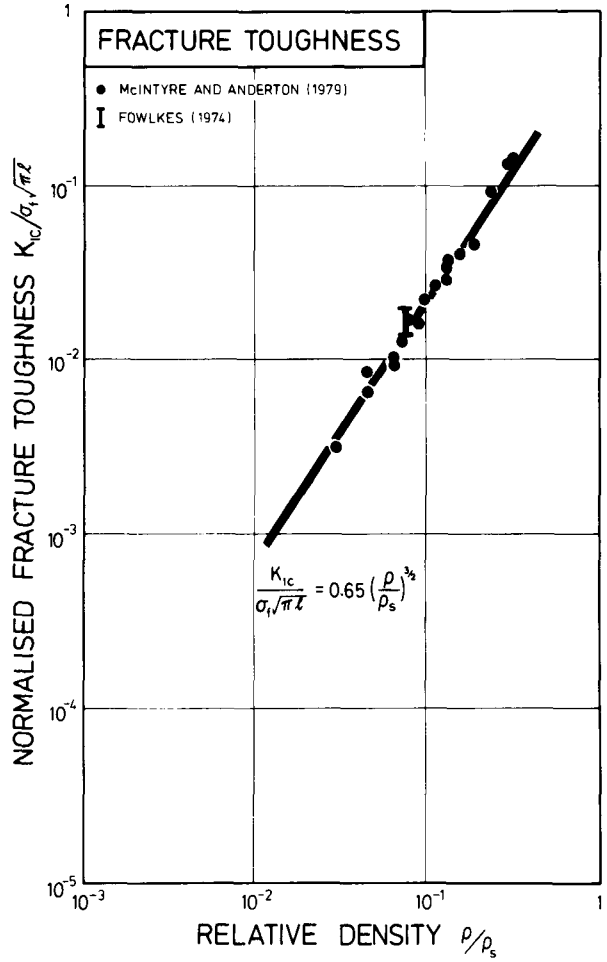

Fig. 14 — The normalized fracture toughness $K_{IC}/\sigma_f \sqrt{\pi l}$ plotted against ρ/ρ_s for crack propagation in brittle foams. The references, in order, are: 27, 28; normalizing constants in Table II.)

IV. OVERALL MECHANICAL RESPONSE: DEFORMATION MAPS

When an elastomeric foam is compressed, it first deforms in a linear-elastic way; then its cells buckle to give nonlinear elasticity; and, finally, the cells collapse completely and the stress rises rapidly as opposing cell walls are forced together. A plastic foam behaves in a somewhat similar way, except that, now, linear elasticity is followed by plastic collapse, and, finally, the forcing together of the cell walls. With brittle foams, progressive crushing can again lead to a plateau, ending when the material is completely crushed. The relevant formuli for open cell foams are summarized in Table III, together with the equivalent results for true closed-cell foams (Figure 3(b)). Most man-made foams behave mechanically as if they had open cells, because surface tension (or other factors) concentrates the solid into the cell edges.

The extent of each phase of deformation depends on the relative density. It is convenient to display this behavior as a *map* with axes of compressive stress and compressive strain, showing the *fields* in which each mechanism is dominant. Superimposed on the fields are *contours of constant (initial) relative density.*

A. *Deformation Map for Elastomeric Foams*

Figure 15 shows a map for elastomeric foams. The linear elastic regime terminates when elastic buckling starts. The boundary of this field (heavy solid line) lies at the strain at which elastic collapse starts. From Eqs. [5] and [7], this strain is:

$$\varepsilon = C_3 = 0.05 \qquad [19]$$

At relative densities above 0.3 the cell walls become so stocky that they can no longer buckle elastically. The curvature of the field boundary is such as to make the linear-elastic loading line for $\rho/\rho_s = 0.3$ tangent to the boundary.

The field of elastic buckling ends at the strain at which the foam finally "bottoms out", or densifies, with a rapid increase of load with displacement. This starts when the folding of the cells is so great that the walls begin to touch. We find that this begins when the foam has been compressed to a new relative density of about 0.5 (that is, the void space occupies half the volume), and it is complete when the foam

Table III. The Equations for Stiffness and Strength of Foams

Property	Open-Cell Foams*	Closed-Cell Foams†
Linear elasticity	$\frac{E}{E_s} = C_2\left(\frac{\rho}{\rho_s}\right)^2$	$\frac{E}{E_s} = B_2\left(\frac{\rho}{\rho_s}\right)^3$
	$C_2 \sim 1$ (Eq. [5])	
Elastic collapse	$\frac{\sigma^*_{el}}{E_s} = C_3\left(\frac{\rho}{\rho_s}\right)^2$	$\frac{\sigma^*_{el}}{E_s} = B_3\left(\frac{\rho}{\rho_s}\right)^3$
	$C_3 \approx 0.05$ (Eq. [7])	
Plastic collapse	$\frac{\sigma^*_{pl}}{\sigma_y} = C_4\left(\frac{\rho}{\rho_s}\right)^{3/2}$	$\frac{\sigma^*_{pl}}{\sigma_y} = B_4\left(\frac{\rho}{\rho_s}\right)^2$
	$C_4 \approx 0.3$ (Eq. [9])	
Creep	$\frac{\dot{\varepsilon}}{\dot{\varepsilon}_0} = C_5\frac{(2n+1)^n}{(n+2)n^n}\left(\frac{C_6\sigma}{\sigma_0}\right)^n\left(\frac{\rho_s}{\rho}\right)^{(3n+1)/2}$	$\frac{\dot{\varepsilon}}{\dot{\varepsilon}_0} = B_5\frac{(2n+1)^n}{(n+2)n^n}\left(\frac{B_6\sigma}{\sigma_0}\right)^n\left(\frac{\rho_s}{\rho}\right)^{2n+1}$
	$C_5 \approx 1$; $C_6 \approx 1.25$ (Eq. [13])	
Brittle crushing	$\frac{\sigma^*_f}{\sigma_f} = C_7\left(\frac{\rho}{\rho_s}\right)^{3/2}$	$\frac{\sigma^*_f}{\sigma_f} = B_7\left(\frac{\rho}{\rho_s}\right)^2$
	$C_7 \approx 0.65$ (Eq. [15])	
Fracture toughness	$K_{IC} = C_8\left(\frac{\rho}{\rho_s}\right)^{3/2}\sigma_f\sqrt{\pi l}$	$K_{IC} = B_8\left(\frac{\rho}{\rho_s}\right)^2\sigma_f\sqrt{\pi l}$
	$C_8 \approx 0.65$ (Eq. [18])	

*In most foams the solid is concentrated into the cell edges; then the open-cell formulae are appropriate. The maps shown in Figures 15 and 17 were constructed using them.

†These equations refer to true, closed-cell foams with no thickening of the cell edges. They are derived by the method given in the text, but using Eqs. [3] in place of Eqs. [1] and [2]. The quantities B_1 to B_2 are dimensionless constants.

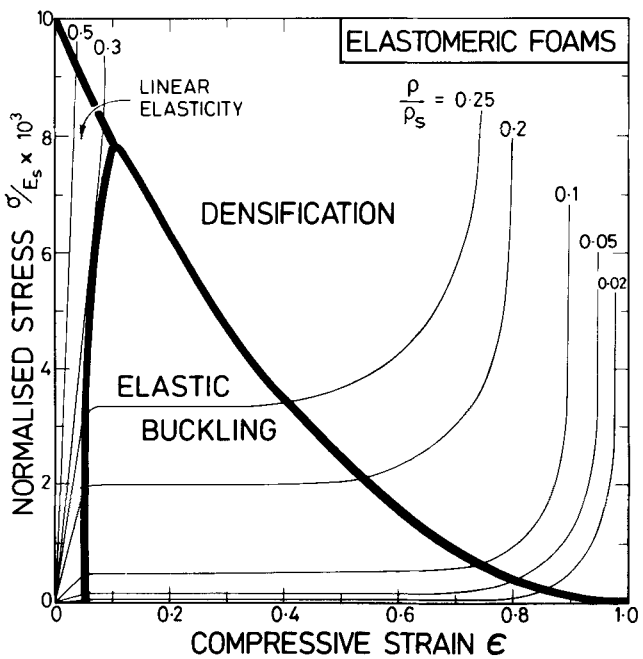

Fig. 15—A deformation-mechanism map for elastomeric foams, for relative densities from 0.02 to 1.

has been compressed to a new relative density of 1 (no void space left).

During elastic buckling the foam compresses axially with no lateral spreading ($\nu = 0$). Then the relative density after a nominal compressive strain* ε is just $(\rho/\rho_s)(1/(1-\varepsilon))$.

*Nominal compressive strain $\varepsilon = (h_o - h)/h_o$ where h_o is the original height and h the height after a compressive strain of ε.

Equating this to 0.5 gives the strain at which densification starts.

$$\varepsilon_s = 1 - 2\frac{\rho}{\rho_s} \qquad [20]$$

and equating it to 1 gives the strain at which densification is complete:

$$\varepsilon_c = 1 - \frac{\rho}{\rho_s} \qquad [21]$$

(where ρ/ρ_s, of course, is the *initial* relative density). Within the elastic buckling field, the stress is related to the density by Eq. [7]; using Eq. [20] gives the equation of the field boundary (heavy solid line) for the start of densification:

$$\varepsilon_s \approx 1 - 10\left(\frac{\sigma}{E_s}\right)^{1/2} \qquad [22]$$

The contours are stress-strain curves for foams of relative density between 10^{-2} and 1. They show a linear elastic regime (Eq. [5]), and a plateau corresponding to elastic buckling (Eq. [7]); they start to bend upward when densification starts (Eq. [22]) and approach a limiting slope of E_s when densification is complete (Eq. [21]). Within the field of elastic buckling the material can exist in two states at almost the same stress (rather like the p-v response of an

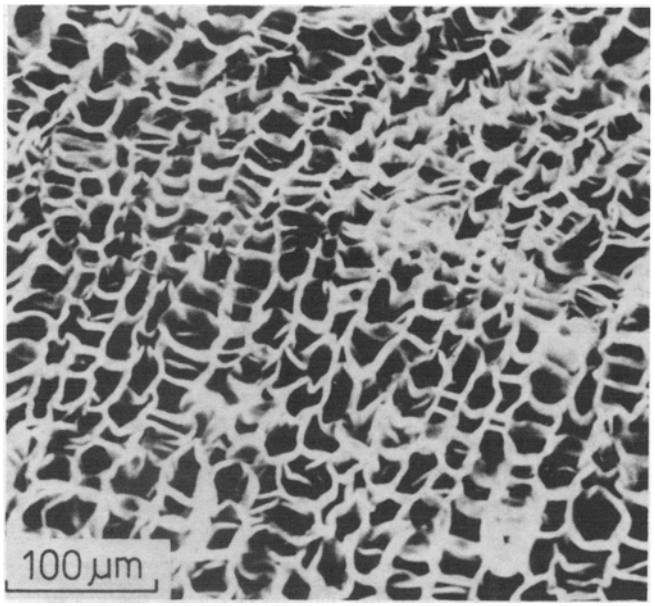

Fig. 16—The progressive collapse of cork, an elastomeric foam.

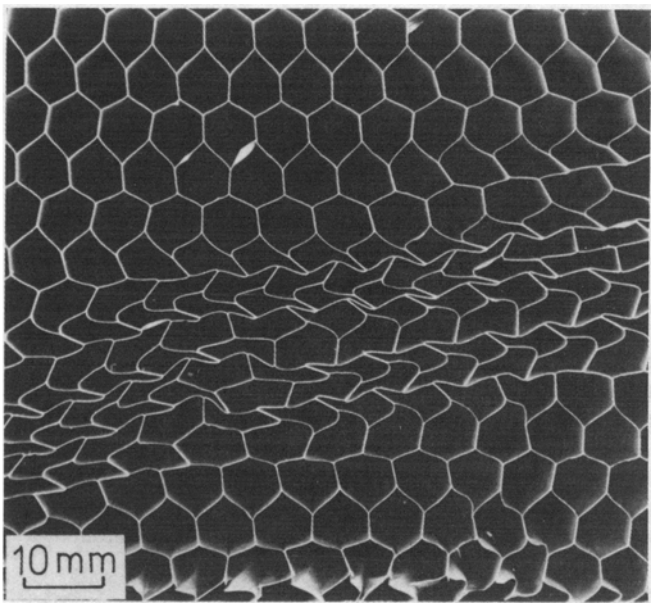

Fig. 18—The progressive collapse of cells in an aluminum honeycomb.

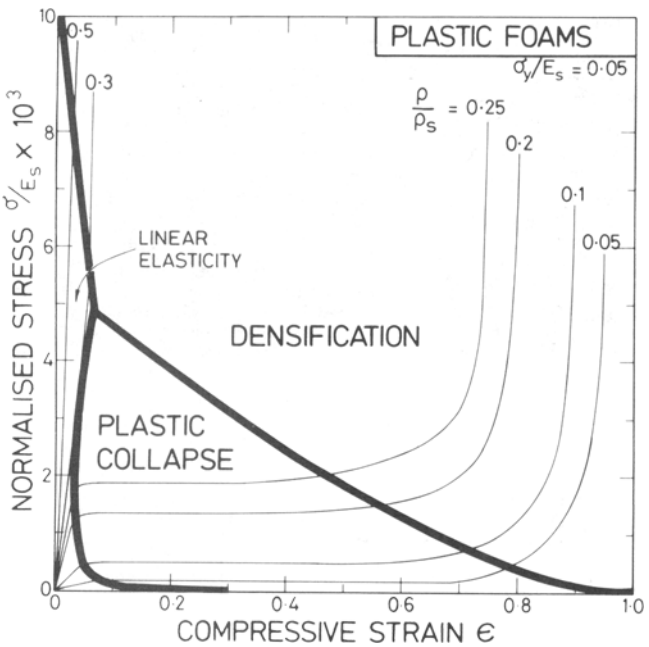

Fig. 17—A deformation-mechanism map for a plastic foam, for which $\sigma_y/E_s = 0.05$, for relative densities from 0.05 to 1.

ideal gas). It collapses in bands which broaden as strain increases: Figure 16, of cork, illustrates this.

The figure describes the overall response of all isotropic foams in compression. Elastomeric foams in tension show roughly linear-elastic response to rupture.

B. *Plastic Foams*

Plastic foams (Figure 17), like the elastic ones, show three regions: linear elasticity, plastic collapse, and densification—though now the strain beyond the linear-elastic regime is not recoverable.

The boundary of the linear-elastic field (heavy line) is obtained from Eqs. [5] and [9]; its equation is:

$$\frac{\sigma}{E_s} = \left(0.3\frac{\sigma_y}{E_s}\right)^4 \frac{1}{\varepsilon^3} \qquad [23]$$

In constructing this map we have taken σ_y/E_s to be 0.05. Next to the linear-elastic field is the field of plastic collapse. As before, two states of strain coexist at almost the same stress, so that complete collapse of part of the structure can occur while the rest is still elastic (Figure 18); the bands of dense material broaden with increasing strain. Densification starts (as before) when the cell walls touch (Eq. [20]) and is complete when the relative density reaches 1 (Eq. [22]). The field boundary (heavy line) defining the start of densification is given, by the arguments leading to Eq. [22] by:

$$\varepsilon = 1 - 4.5\left(\frac{\sigma}{E_s}\Big/\frac{\sigma_y}{E_s}\right)^{2/3} \qquad [24]$$

Superimposed on the fields are stress-strain curves for foams of initial relative density between 0.05 and 1. They show a linear elastic regime (Eq. [5]) and a plateau corresponding to plastic collapse (Eq. [9]); they start to bend upward when densification starts (Eq. [24]) and reach a limiting slope of E_s when densification is complete (Eq. [21]).

The figure shows the overall response of isotropic, plastic foams compression. It is less general than the map for elastomeric foams because it must be constructed for a particular value of σ_y/E_s, but the equations show that the boundaries are not very sensitive to its value, and, for a given material, the diagram shows the behavior for all densities.

The behavior of plastic foams in tension resembles that in compression, truncated by fracture.

C. *Rigid Foams*

Rigid foams show linear-elastic behavior (Eq. [5]) to fracture. In compression, the foam crushes at constant stress

(Eq. [15]), and since the crushing equation has the same form as that for plastic collapse, the behavior will resemble that of Figure 17. If the foam is contained, it will densify at the strain given approximately by Eq. [24], with σ_y/E_s replaced by σ_f/E_s.

In tension, linear elastic behavior is truncated by fast, brittle fracture at the stress given by Eq. [17].

V. APPLICATIONS

This approach to the mechanics of cellular solids has many applications. It helps in design and selection of materials for cushions and packaging. It contributes to the understanding of the mechanics of natural materials such as wood,[35] and it gives a foundation for the design with foams in load-bearing structures like sandwich panels.[36] We conclude with three examples in each of which the unique properties of cellular solids are, or could be, exploited.

A. *The Anisotropy of Cork*

Cork has a remarkable combination of properties. It is light yet resilient; it is an excellent insulator for heat and sound, it has a high coefficient of friction; and it is impervious to liquids, is chemically stable and fire resistant. It owes its special properties to its chemical composition, quite different from that of wood, and to its cellular structure.[37]

Cork is a closed-cell foam with a specific gravity of about 0.15. Figure 19 shows that the cells are about 30 μm across, and that the cell shape is anisotropic: the cells are hexagonal prisms, with the prism axis of each cell parallel to a common direction. The asymmetry of the shape makes the cork properties anisotropic: Young's modulus in the plane normal to the prism axis is constant, but differs from that parallel to the prism axis. Because of the cell shape, compression down the prism axis produces no lateral expansion: Poisson's ratio in this direction is zero.

Since Roman times, cork has been used to stop wine bottles; Horace speaks of it in his Odes.[38] Today, despite attempts to replace it by plastics, real cork remains the only choice of the true connoisseur of wines. Why does cork make such good stoppers?

Part of the reason is the chemical stability. But part is the special elastic behavior of a cellular solid. Its stress-strain curve is shown in Figure 20: it has exactly the shape expected of an elastomeric foam. In cutting a cork, it obviously makes sense to make the axis of the cork parallel to the axis of symmetry of its structure: then the cork presses uniformly on the neck of the bottle (because the radial Young's modulus is constant), and it can be inserted easily (because Poisson's ratio is zero for compression down the prism axis).

The reasoning is sound, but there is a problem. Natural cork contains tubular channels or *lenticels* to allow gases to pass through to the wood beneath; they are visible on any piece of cork (*e.g.*, Figure 21). The lenticels lie parallel to the prism axis, so corks cut parallel to this axis would leak. This is why cheap corks are cut with the lenticels (and axis of symmetry) *across* the cork, as shown in Figure 21(a). But when good wine is to be bottled, only the best will do, and the best requires the proper alignment of cork. The solution is shown in Figure 21(b): the cork is made of two or more slices, properly aligned, and bonded together so that the lenticels do not connect, thus using the elastic anisotropy of the structure to maximum advantage.

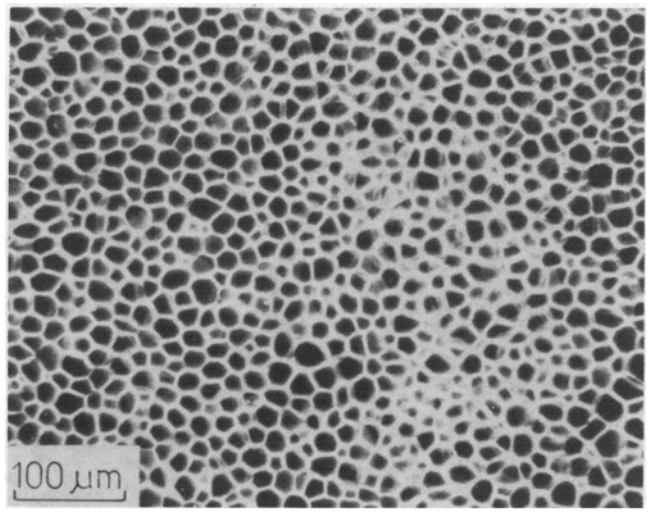

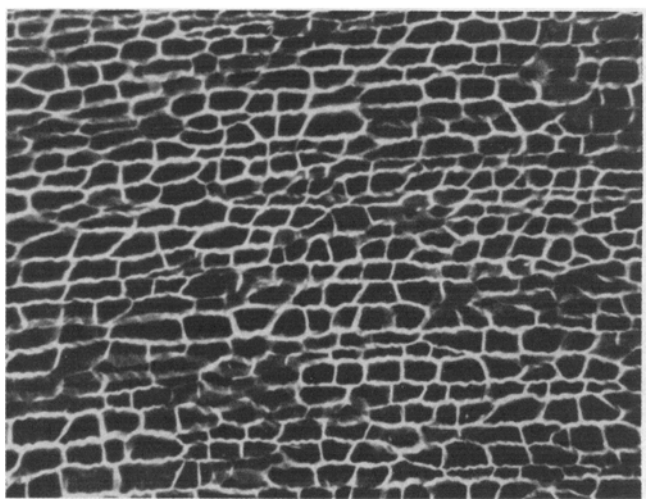

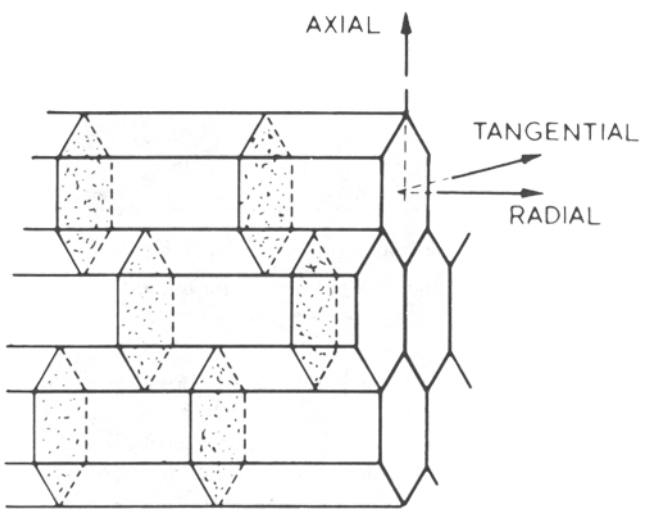

Fig. 19—The cells in cork. They are hexagonal prisms. The cork properties have hexagonal symmetry. The upper section is cut normal to the radial direction; the lower one is cut normal to the axial direction.

This is just one example of the use of the anisotropy of a cellular solid. Design with wood, an exceedingly anisotropic material, is another. At present, most man-made

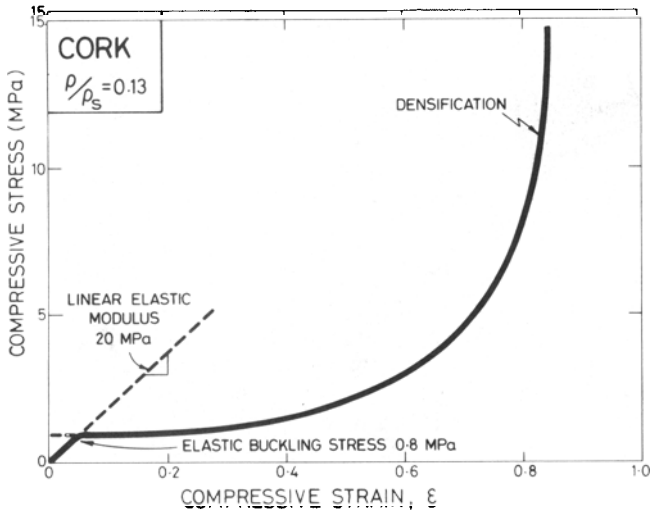

Fig. 20 — The stress-strain curve of cork. It follows the pattern shown in the map of Fig. 15.

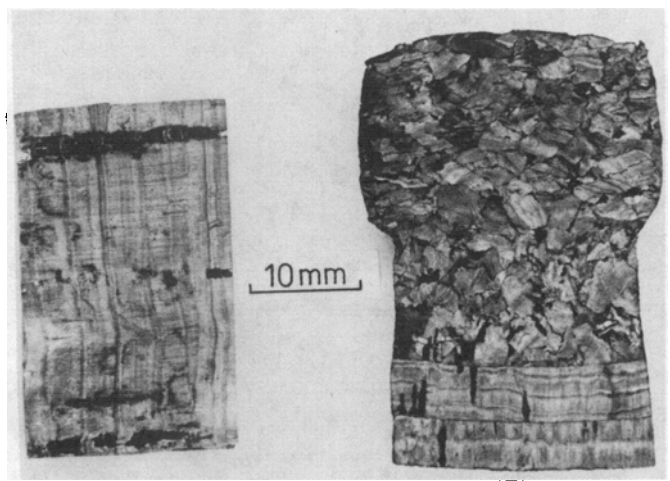

Fig. 21 — Sections through corks. The axis of symmetry of the cork structure is parallel to the lenticels (dark lines).

foams are isotropic. The potential for designing anisotropy into foams, and exploiting it in packaging, soles for shoes, seating or crash padding, is considerable.

B. *Cellular Solids in Nature: Scaling of Trees*

Why are cellular solids so common in nature? The size and scale of a tree is determined by the mechanical properties of the materials of which it is made. A tall and spreading tree has a clear advantage in exposing more of its leaves to light (Figure 22), but if the branches are too long (for their diameter) they will bend too far, defeating their purpose of carrying the leaves out of the shade of higher branches. If the trunk is too tall (for its girth) it will buckle elastically, as trees do when heavy snow overloads them. It has long been known that the height h of a tree is related to the diameter, d, of its trunk, by Kleiber's law:[39]

$$h \propto d^{2/3} \qquad [25]$$

and the branch length, l, bears the same relation to the branch diameter.[39] This law follows directly from these mechanical criteria:[40] if the force Mg due to the mass $M = \pi d^2 h \rho$ of the tree is equated to the buckling force

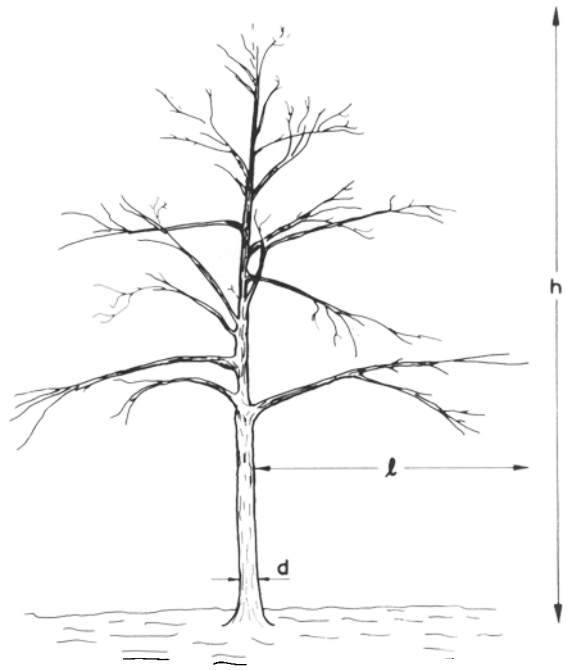

Fig. 22 — The scale of a tree. Cellular materials permit a taller tree.

(Eq. [6]), Eq. [25] is obtained immediately; and if the droop δ (Eq. [4]) of a branch under its self-weight is set equal to a fraction of its length, the same result is found. The same procedure gives the height and spread of a tree in terms of the mass of material it contains. The result is:

$$h \quad \text{and} \quad l \propto \left(\frac{M}{g}\right)^{1/4}\left(\frac{E}{\rho^2}\right)^{1/4} \qquad [26]$$

(where g is the acceleration due to gravity). The most efficient use of material, then, is that which distributes it such that E/ρ^2 is a maximum.

This is where a cellular structure works so well. Table IV compares E, E/ρ, and $E^{1/2}/\rho$ for the cellulose-hemicellulose-lignin composite of which the cell walls of wood are made, and the wood itself. The modulus of wood (along the grain) is much less than that of the cell wall; the specific modulus is about the same as that of the cell wall; but the value of $E^{1/2}/\rho$ is much greater. A cellular tree can grow to roughly twice the height of a solid one, using the same quantity of cellulose. This efficiency in material use must be one of the reasons cellular structures are so common in nature.

C. *Sandwich Construction*

Higher forms of life have more complicated structures. The bones of mammals are an example: they have a cellular interior, but they also have a solid outer skin; they are a sort of sandwich panel (Figures 2(d), 2(f), and (23)).

Sandwich panels are increasingly used in engineering.[42] Cheap doors are a sandwich of flimsy plywood with a paper honeycomb. Modern refrigerators are only half the weight of older ones, partly because the sides and door are made of a thinner sheet steel, bonded to polyurethane foam which gives both stiffness and insulation. Yacht hulls and decks can be made of thin fiberglass skins bonded to a foam or to balsa wood. These ideas derive from the aerospace industry: balsa-filled sandwiches were first used during World

Table IV. Moduli and Specific Moduli for Woods in Units of Those of the Cell Walls

	E	E/ρ	$E^{1/2}/\rho$
Solid tree (Cellulose/Lignin/ Hemicellulose)	1	1	1
Cellular tree, $\rho/\rho_s = 0.1 \rightarrow 0.5$	0.1 to 0.5	1	2 to 4

Data for moduli and densities from Dinwoodie.[41]

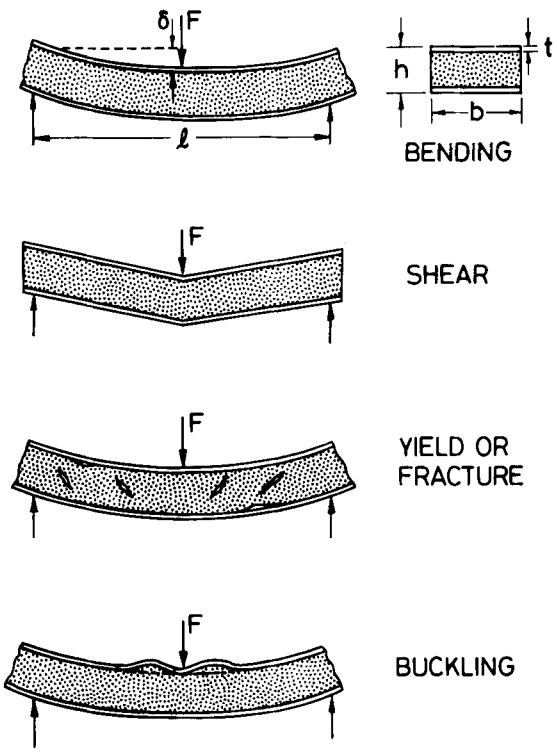

Fig. 23—The modes of deformation and failure of a sandwich panel. The panel stiffness may be controlled by bending or shear, and failure may be by the failure of the skin or the core.

War II, and metal and polymer sandwiches form parts of the airframe, wing structure, and flooring of most modern planes. Skis are perhaps the most highly-tuned sandwiches of all: in many designs, the right combination of longitudinal and flexural stiffness is achieved by a foam-filled sandwich. And sandwiches are common in nature: bone, the wing casing of beetles, the cuttle-bone of the cuttle fish.

The aim, in every case, is a structure with the minimum weight for a given stiffness or strength. It is interesting to ask whether these natural and man-made structures are *optimal,* that is, whether they achieve the minimum weight for a given stiffness or strength. The problem is complicated. There are many variables—the skin thickness, density and strength, the core thickness and its density and strength—and there are several failure modes: fracture, crushing, skin buckling, or tensile fracture (Figure 23). The full answer is not yet known—though there are some indications that bone may be close to the optimum, and, of course, there are enormous advantages to the animal to being optimized. Some man-made panels have been optimized approximately by empirical methods.

The reason that the question is incompletely answered is that the properties of the cellular core had not, until now, been analyzed fully. The results assembled in this paper show, I think, that the foam itself is now well understood. We are now in a position to analyze natural and man-made sandwiches more completely.

ACKNOWLEDGMENTS

We wish to acknowledge many helpful discussions with Professor K. E. Easterling, Professor T. McMahon, Dr. C. R. Calladine, Dr. W. C. Nixon, Dr. P. Echlin, and Mr. George Woodly, of Ciba-Geigy. We particularly wish to thank Mr. John Godlonton for technical assistance, and to acknowledge the financial support of the British Science and Engineering Research Council.

REFERENCES

1. L. J. Gibson: Ph.D. Thesis, Engineering Department, Cambridge University, 1981.
2. L. J. Gibson, M. F. Ashby, G. S. Schajer, and C. I. Robertson: *Proc. R. Soc. Lond.*, 1982, vol. A382, p. 25.
3. M. R. Patel and I. Finnie: *J. Materials*, 1970, vol. 5, p. 909.
4. F. K. Abd. El Sayed, R. Jones, and I. W. Burgess: *Composites*, 1979, vol. 10, p. 209.
5. A. N. Gent and A. G. Thomas: *J. Appl. Polymer Sci.*, 1959, vol. 1, p. 107.
6. A. M. Gent and A. G. Thomas: *Rubber Chem. Technol.*, 1963, vol. 36, p. 597.
7. W. L. Ko: *J. Cell. Plastics*, 1965, vol. 1, p. 45.
8. J. M. Lederman: *J. Appl. Polymer Sci.*, 1971, vol. 15, p. 693.
9. G. Menges and F. Knipschild: *Polymer Eng. Sci.*, 1975, vol. 15, p. 623.
10. L. J. Gibson and M. F. Ashby: *Proc. R. Soc. Lond.*, 1982, vol. A382, p. 43.
11. S. Baxter and T. T. Jones: *Plastics Polymers*, 1972, vol. 40, p. 69.
12. P. J. Phillips and N. R. Waterman: *Polymer Engng. Sci.*, 1974, vol. 4, p. 67.
13. D. R. Moore: (1980) "The use of glass in engineering", Design Council Guide 05, Oxford, Univ. Press, 1975.
14. R. Chan and M. Nakamura: *J. Cell. Plastics*, 1969, vol. 5, p. 112.
15. C. A. Brighton and A. E. Meazey: "Expanded polyvinyl chloride," in "Expanded Plastics—Trends in Performance Requirements"—A Micro Symposium organized by Q.M.C. Industrial Research Ltd., September 25, 1973, London.
16. M. Wilsea, K. L. Johnson, and M. F. Ashby: *Int. J. Mech. Sci.*, 1975, vol. 17, p. 457.
17. J. B. Walsh, W. F. Brace, and A. W. England: *J. Am. Ceram. Soc.*, 1965, vol. 48, p. 605.
18. Pittsburgh-Corning Inc., Foamglass Data Sheets, 1982.
19. V. A. Matonis: S.P.E. J1, September 1964, p. 1024.
20. P. Barma, M. B. Rhodes, and R. Salovey: *J. Appl. Phys.*, 1978, vol. 49, p. 4985.
21. P. H. Thornton and C. L. Magee: *Metall. Trans. A*, 1975, vol. 6A, p. 1253.
22. P. H. Thornton and C. L. Magee: *Metall. Trans. A*, 1975, vol. 6A, p. 1801.
23. R. K. Traeger: *J. Cell. Plastics*, 1967, vol. 3, p. 405.
24. M. C. Shaw and T. Sata: *Int. J. Mech. Sci.*, 1966, vol. 8, p. 469.
25. J. A. Rinde: *J. Appl. Poly. Sci.*, 1970, vol. 14, p. 1913.
26. K. C. Rusch: *J. Appl. Poly. Sci.*, 1970, vol. 14, p. 1263.
27. A. McIntyre and G. E. Anderton: *Polymer*, 1979, vol. 20, p. 247.
28. C. W. Fowlkes: *Int. J. Fracture*, 1974, vol. 10, p. 99.
29. W. F. Roff and J. R. Scott: *Fibres, Films, Plastics and Rubbers—A Handbook of Common Polymers*, Butterworths, London, 1971.
30. C. A. Harper: *Handbook of Plastics and Elastomers*, New York, NY, McGraw-Hill, 1975.
31. B. J. Lazan: *Damping of Materials and Members in Structural Mechanics*, Oxford, Pergamon Press, 1968.
32. F. W. Billmeyer: *Textbook of Polymer Science*, 2nd edn., New York, NY, Wiley Interscience, 1971.
33. M. J. Bonnin, C. M. R. Dunn, and S. Turner: *Plastics Polymers*, 1969, vol. 37, p. 517.

34. D. S. Oliver: (1980) "The Use of Glass in Engineering", Design Council Guide 05, Oxford Univ. Press, 1975.
35. K. E. Easterling, R. Harrysson, L. J. Gibson, and M. F. Ashby: *Proc. R. Soc. Lond.*, 1982, vol. A383, p. 31.
36. L. J. Gibson: to be published, 1984.
37. L. J. Gibson, K. E. Easterling, and M. F. Ashby: *Proc. R. Soc.*, 1981, vol. A377, p. 99.
38. Q. Horace: *Odes*, 27 B.C., Book III, ode 8, line 10.
39. M. Kleiber: *Hilgardia*, 1932, vol. 6, p. 315.
40. T. McMahon: *Science*, 1973, vol. 179, p. 1201.
41. J. M. Dinwoodie: "Timber, its Nature and Behaviour", New York, NY, van Nostrand, 1981.
42. H. G. Allen: "Analysis and Design of Structural Sandwich Panels", Pergamon Press, Oxford, 1969.